First Principles Explanation of the Positive Seebeck Coefficient of Lithium

Bin Xu[1,2,*] and Matthieu J. Verstraete[1,2]
[1]Département de Physique, Université de Liège, Allée du 6 Août 17, B-4000 Sart Tilman, Belgium
[2]European Theoretical Spectroscopy Facility

(Received 25 November 2013; revised manuscript received 19 March 2014; published 14 May 2014)

Lithium is one of the simplest metals, with negative charge carriers and a close reproduction of free-electron dispersion. Experimentally, however, Li is one of a handful of elemental solids (along with Cu, Ag, and Au) where the sign of the Seebeck coefficient (S) is opposite to that of the carrier. This counterintuitive behavior still lacks a satisfactory interpretation. We calculate S fully from first principles, within the framework of Allen's formulation of Boltzmann transport theory. Here it is crucial to avoid the constant relaxation time approximation, which gives a sign for S which is necessarily that of the carriers. Our calculated S are in excellent agreement with experimental data, up to the melting point. In comparison with another alkali metal, Na, we demonstrate that within the simplest nontrivial model for the energy dependency of the electron lifetimes, the rapidly increasing density of states (DOS) across the Fermi energy is related to the sign of S in Li. The exceptional energy dependence of the DOS is beyond the free-electron model, as the dispersion is distorted by the Brillouin zone edge; this has a stronger effect in Li than other alkali metals. The electron lifetime dependency on energy is central, but the details of the electron-phonon interaction are found to be less important, contrary to what has been believed for several decades. Band engineering combined with the mechanism exposed here may open the door to new "ambipolar" thermoelectric materials, with a tunable sign for the thermopower even if either n- or p-type doping is impossible.

DOI: 10.1103/PhysRevLett.112.196603 PACS numbers: 72.15.Jf, 72.10.Di, 72.15.Eb, 72.15.Lh

Thermoelectricity (TE) has drawn much attention over the past century [1,2] as an effective way of producing electricity from heat energy, or vice versa. In addition to applications in waste heat recovery, the reversible functionality of TE materials also enables heating and refrigeration within the same unit. Spot cooling [3] of computer processors can be achieved with TE devices of small size and without moving parts. The efficiency of current thermoelectric devices is relatively low compared to, e.g., thermal engines, which limits their applications [1]. In the search for a good thermoelectric material, a large Seebeck coefficient (S) is one of the central components in the figure of merit, where it appears squared. Most advances in TE, however, have targeted the simpler tasks of lowering the thermal conductivity [4] or optimizing the electron density of states [5]. The magnitude of S is also important in other applications, e.g., for thermal sensors [6]. Though S can be measured straightforwardly in experiment and calculated theoretically within certain approximations, a complete microscopic understanding and paths for systematic improvement of S are still lacking. The most common approach is to consider a constant averaged relaxation time for the electrons (τ). The relaxation time approximation (RTA) works in a surprisingly large number of cases, but has little formal justification; we expose some more of its limitations below.

Materials with n-type carriers should yield negative S, as electrons diffuse from the high-temperature side to the low-temperature side. This is not the case for the monovalent metal Li at ambient pressure. It has been known for a long time that lithium exhibits positive S from low to high temperatures, through a martensitic transformation at 77 K [7] and melting at 454 K [8–11]. This is in contrast to most simple metals, in particular, to other alkali metals [12–14]. An explanation was proposed by Robinson nearly half a century ago based on a nearly free-electron model, where the positive Seebeck of Li was attributed to the energy variance of the mean free path around the Fermi energy [15], due to an unusual energy dependence of the electron-phonon interaction [16]. These calculations adopted model interactions for the scattering of electrons by lattice vibrations, which relied on empirical parameters. On the other hand, a controversial argument was proposed by Jones in the 1950s that the positive Seebeck in monovalent metals is due to the significant deviation from the free-electron density of states (DOS), because part of the Fermi surface lies close to the Brillouin zone boundary [17]. No actual calculation was carried out to verify this hypothesis. MacDonald also pointed out that Li may depart considerably from a simple free-electron model [13]. Ziman ascribed the large positive humps of S in alkali metals (except Na and K) at low temperature to phonon drag. The phonon drag contribution for Li is very slight, and peaks around 80 K [12]. In this Letter, we revisit the anomalous sign of S in Li through fully *ab initio* calculations within the framework of Boltzmann's transport theory. To understand the positive sign of S in Li, we also

explore the S of sodium metal, for a comparative analysis. Contrary to Robinson's hypothesis, while consistent with that of Jones, we indeed find significant deviation from the free-electron model in Li, and that the electron-phonon interaction is not primarily responsible for the positive S. Furthermore we show that, within a simple model for the energy-dependent lifetime $\tau(\epsilon)$, the spectral conductivity (a purely electronic quantity) determines the sign of S. We do not treat the phonon drag contribution, which can be dominant below 50–100 K, but show that the diffusive contribution is enough to describe the main variation of $S(T)$.

To calculate the Seebeck coefficient, we adopt the lowest-order variational approximation (LOVA) to the Boltzmann transport equation [18]. For S it is crucial to include explicitly inelastic contributions and Fermi smearing effects. These are beyond the commonly used elastic version of the LOVA [18,19], which leads to $S = 0$. In the LOVA,

$$S_{\alpha\beta} = (\pi k_B/\sqrt{3}e)\sum_{\gamma}(Q_{01})_{\alpha\gamma}(Q_{11}^{-1})_{\gamma\beta}, \tag{1}$$

where $(Q_{nn'})_{\alpha\beta}$ is the scattering operator for Cartesian directions ($\alpha, \beta = x, y, z$), expressed in Allen's basis set (indices n, n'), and e is the absolute value of the electron charge. The basis set is separated into $\mathbf{k}$-dependent "Fermi-surface harmonics" (FSH) and energy-dependent polynomials (see below). In the LOVA one uses only the lowest nonzero FSH, which is simply a normalized Fermi velocity, viz., $F_\alpha(\mathbf{k}) = v_\alpha(\mathbf{k})/v_\alpha(\epsilon_F)$. The normalization is given by $v_\alpha^2(\epsilon) = [\sum_{\mathbf{k}} v_\alpha^2(\mathbf{k})\delta(\epsilon_{\mathbf{k}} - \epsilon)]/N(\epsilon)$, where $N(\epsilon)$ is the density of electronic states.

The scattering operators are calculated as

$$\begin{aligned}(Q_{nn'})_{\alpha\beta} = {} & \frac{2\pi V_{\text{cell}} N(\epsilon_F)}{\hbar k_B T}\int d\epsilon d\epsilon' d\omega \sum_{s,s'=\pm 1} f(\epsilon)[1 - f(\epsilon')] \\ & \times \{[N(\omega) + 1]\delta(\epsilon - \epsilon' - \hbar\omega) + N(\omega)\delta(\epsilon - \epsilon' + \hbar\omega)\} \\ & \times \alpha_{\text{tr}}^2 F(s, s', \alpha, \beta, \epsilon, \epsilon', \omega) J(s, s', n, n', \epsilon, \epsilon'),\end{aligned} \tag{2}$$

where ϵ, ϵ' are electron energies relative to the Fermi level ϵ_F, ω is a phonon frequency, V_{cell} is the unit cell volume, f and N are the Fermi-Dirac and Bose-Einstein distributions at temperature T, respectively. The transport spectral function $\alpha_{\text{tr}}^2 F$ is analogous to the Eliashberg spectral function for superconductivity, but weighted by contributions from electron velocities. Among all the mechanisms that affect the electronic transport, here we only consider the electron-phonon coupling (EPC), which is dominant for most materials except at very low temperatures. See the Supplemental Material [20] for definitions and an overview of Allen's formalism. For the sign of S a crucial quantity is the joint function $J(s, s', n, n', \epsilon, \epsilon')$ in Eq. (2),

$$\frac{1}{4}\left[\frac{\zeta_n(\epsilon)}{N(\epsilon)v(\epsilon)} + s\frac{\zeta_n(\epsilon')}{N(\epsilon')v(\epsilon')}\right]\left[\frac{\zeta_{n'}(\epsilon)}{N(\epsilon)v(\epsilon)} + s'\frac{\zeta_{n'}(\epsilon')}{N(\epsilon')v(\epsilon')}\right],$$

composed of energy polynomials $\zeta_n(\epsilon)$, with $\zeta_0 = 1$ and $\zeta_1 = \sqrt{3}\epsilon/\pi k_B T$.

The EPC matrix elements, phonons, and electronic velocities are calculated within density functional perturbation theory (DFPT) [21,22], carried out using the ABINIT package [23]. The exchange and correlation functional is treated with the local density approximation. For bcc Li, an unshifted $36 \times 36 \times 36$ $\mathbf{k}$-point grid and $12 \times 12 \times 12$ $\mathbf{q}$-point grid are employed, ensuring good convergence for transport properties. For bcc Na, an unshifted $\mathbf{k}$ grid of $24 \times 24 \times 24$ is found to be sufficient for our comparisons. For the ground state and DFPT calculations a "cold smearing" function [24] of width 0.04 hartree is used to improve $\mathbf{k}$-grid convergence. The plane-wave basis functions with kinetic energies up to 20 hartree are used in both systems.

For comparison, the Seebeck coefficient is also calculated within the constant relaxation time approximation, using the BOLTZTRAP code [25]. This approach has often been adopted in theoretical studies of thermoelectric properties. In the RTA,

$$S_{\alpha\beta} = -\frac{1}{eT}\frac{\int \sigma_{\alpha\beta}(\epsilon)(\epsilon - \epsilon_F)(-\frac{\partial f}{\partial \epsilon})d\epsilon}{\int \sigma_{\alpha\beta}(\epsilon)(-\frac{\partial f}{\partial \epsilon})d\epsilon}, \tag{3}$$

where $\sigma_{\alpha\beta}(\epsilon)$ is $e^2\tau\sum_{\mathbf{k}} v_\alpha(\mathbf{k})v_\beta(\mathbf{k})\delta(\epsilon - \epsilon_{\mathbf{k}})$, with τ the constant relaxation time [which cancels out in Eq. (3)].

The calculated S, together with the experimental data, are shown in Fig. 1. Within the temperature range where the bcc phase is stable, our prediction using the variational approach (VA) agrees very well with the measured S, except the older data from Bidwell, which deviates significantly from other experimental values. The excellent agreement on the magnitude and temperature dependence of S also implies that electron-phonon coupling is the main, if not sole, contribution to the electronic transport properties in bcc Li. This can also be seen from the agreement with measured data [26] in electrical resistivity (see Supplemental Material, Fig. 2 [20]). On the other hand, S calculated with a constant relaxation time (red dashed line in Fig. 1) is negative for all temperatures. This is a clear and qualitative failure of the constant RTA. In the case of Na (Fig. 2), both theoretical predictions are consistent with the experimental sign of S, i.e., negative. Comparing to the magnitude of room-temperature S (~ -6 μV/K) in experiments [9,11], the VA result (-5.42 $\mu V/K$) is in good agreement, whereas the constant RTA (-3.09 μV/K) underestimates by nearly 50%. The sign and order of magnitude of S beyond the melting temperature appear to be preserved, though with a jump for Li. This suggests that the conduction mechanism stays fairly simple even after

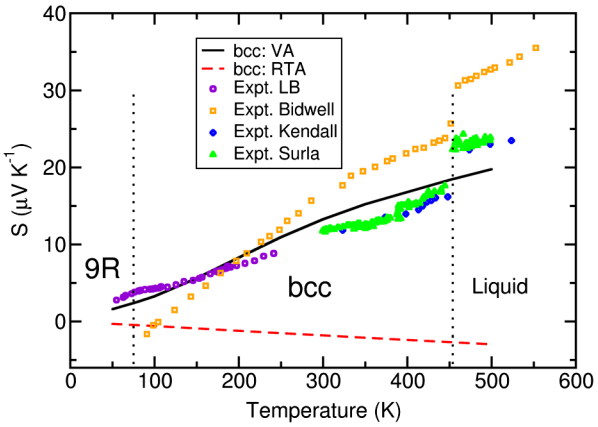

FIG. 1 (color online). Seebeck coefficient of Li, as a function of temperature. Black solid line is the calculated S of bcc Li using the variational approach (extended to the temperature where 9R or liquid phase becomes stable experimentally), and the red dashed line denotes calculated result of bcc Li with constant τ from the BOLTZTRAP code. Discrete points are experimental data from LB (Landolt-Börnstein database) [11], Bidwell [8], Kendall [9], and Surla *et al.* [10]. The vertical dotted lines denote the temperatures of 9R-to-bcc phase transition and melting point.

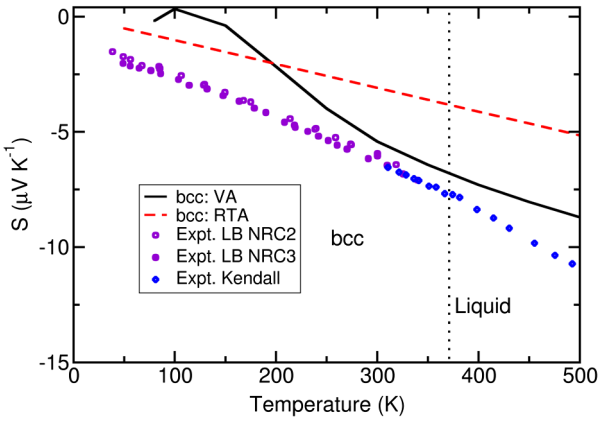

FIG. 2 (color online). Seebeck coefficient of Na, as a function of temperature. Black solid line is the calculated S of bcc Na using the variational approach (extended beyond the experimental melting point), and the red dashed line denotes the calculated result of bcc Na with constant τ. Discrete points are experimental data from Kendall [9] and LB (Landolt-Börnstein database) [11]. The vertical dotted line denotes the temperature of the melting point.

melting. The present methods (Boltzmann transport) are strongly dependent on a solid and crystalline reference phase. Going beyond will require explicit molecular dynamics simulations coupled with a Kubo or other approach to extract the Seebeck coefficient (similar to Ref. [27] for the conductivity of liquid Fe). For further justification of the variational approach, the Seebeck coefficient of K is also calculated (see Supplemental Material, Fig. 3 [20]), which agrees well with measured S; K turns out to be a "normal" Alkali metal similar to Na.

To understand the positive sign of S in Li, we perform a comparative analysis with Na (see Supplemental Material for details [20]). According to Eq. (1), the sign of S is determined by the sign of Q_{01}. The sign of Q_{01} comes from the integral of $\alpha_{\mathrm{tr}}^2 F$ and J_{01} over the electron energy $\int d\epsilon$. The energy dependence of J_{01} alone favors the negative sign of S, for both Li and Na. The different signs of S in Li and Na originate from the energy dependence of $\alpha_{\mathrm{tr}}^2 F$. To examine Robinson's hypothesis [15,16] that positive S in Li is caused by the unusual energy dependence of electron-phonon interactions, we set the electron-phonon coupling matrix to a constant ($g_{\mathbf{k}\mathbf{k}'} = 1$). A positive value of S is again obtained for Li, and negative for Na. Since the normalized function $F(\mathbf{k})$ has a very weak dependence on the energy, the strong energy dependence of $\alpha_{\mathrm{tr}}^2 F(\epsilon)$ in Li is due to the integration weights $\delta(\epsilon_{\mathbf{k}} - \epsilon)$ [see Supplemental Material, Eq. (1) [20]], which is essentially the density of states.

We infer that the sign of S is determined by the energy dependence of the electron lifetime. This can also be seen from the RTA point of view. According to Eq. (3), as $-\partial f/\partial \epsilon$ is positive and symmetric about the Fermi level ϵ_F, the sign of S is determined by the energy dependence of $\sigma(\epsilon)$. Increasing $\sigma(\epsilon)$ yields negative S, and vice versa. For a cubic system, without anisotropy, $\sigma(\epsilon)$ consists of $v^2(\epsilon)$ and $\tau(\epsilon)$. We have shown that constant RTA yields negative S for Li (Fig. 1), so the energy dependence of $\tau(\epsilon)$ is crucial.

If the EPC is featureless, the energy dependence of the electron-phonon scattering rate $1/\tau(\epsilon)$ is proportional to the density of states [28,29]. The electron DOS $N(\epsilon)$ of Li and Na are illustrated in Fig. 3(a). As the sign of S does not change with temperature for Li or Na, we choose $T =$ 300 K for demonstration. In general, a span of $\epsilon_F \pm 8k_B T$ is sufficient to capture the substantial contributions to the transport properties (of S, ρ, etc.). Near the Fermi level, the DOS of Na varies slowly and does not deviate much from the free-electron description. However, Li exhibits a significantly increasing DOS across ϵ_F, until the band reaches the boundary of the Brillouin zone at the N point. For $v^2(\epsilon)$, i.e., $\sum_{\mathbf{k}} v_x(\mathbf{k}) v_x(\mathbf{k}) \delta(\epsilon - \epsilon_{\mathbf{k}})$, Na still shows the free-electron-like linear energy dependence near ϵ_F, but with a much larger slope than Li [Fig. 3(b)]. The variation of $v^2(\epsilon)$ in Li approaches a plateau just after ϵ_F. Again this behavior deviates qualitatively from the free-electron model, where a linear dependence is expected. Combining these two factors, as shown in Fig. 3(c), an increasing $v^2(\epsilon)/N(\epsilon)$ is obtained for Na for the considered energy range around ϵ_F, whereas it is decreasing for Li. At elevated temperatures, although $v^2(\epsilon)/N(\epsilon)$ no longer decreases monotonically for Li due to the larger energy span, the sign of S is unaffected because the major contribution is still from electrons with energies close to the Fermi level.

The relationship between the sign of S and the energy dependence of conductivity can also be seen from the Mott relation, i.e.,

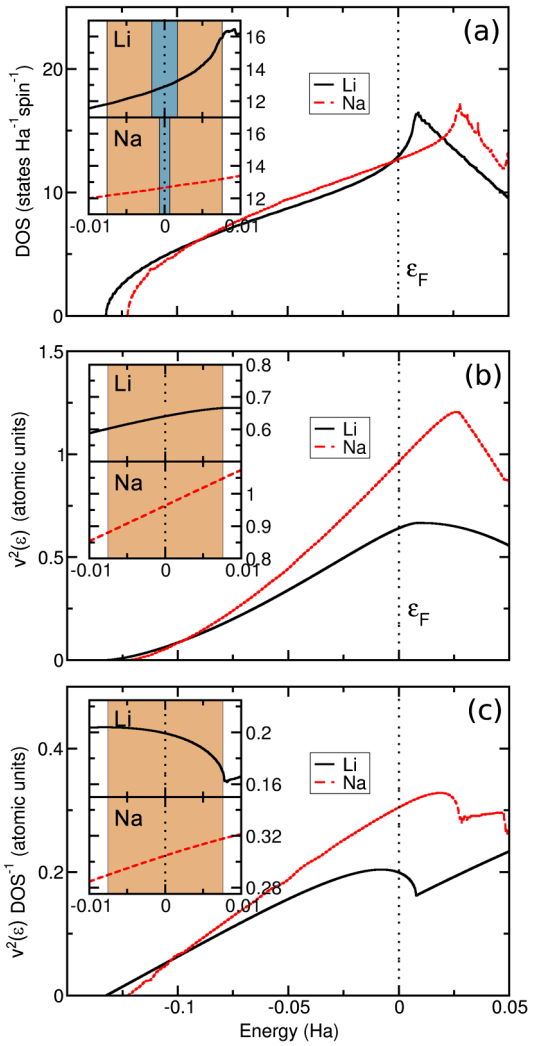

FIG. 3 (color online). (a) Density of states, (b) square of the velocity (energy spectrum), (c) square of the velocity (energy spectrum) divided by the corresponding density of states of Li (solid black line) and Na (dashed red line). The vertical dotted line denotes the Fermi energy. The insets show a zoom around ϵ_F. The orange shaded region covers $\epsilon_F \pm 8k_BT$ with $T = 300$ K. The blue shaded region (darker) shows $\epsilon_F \pm \omega_m$, where ω_m is the maximum energy for phonons.

$$S = -\frac{\pi^2 k_B^2 T}{3e}\left[\frac{1}{\sigma}\frac{d\sigma(\epsilon)}{d\epsilon}\right]_{\epsilon=\epsilon_F}. \quad (4)$$

As a qualitative estimation, if Drude's formula $\sigma = ne^2\tau/m^*$ is adopted for the conductivity and, again, the relaxation time τ is taken to be inversely proportional to the DOS, the energy dependencies from the charge carrier density and τ are approximately balanced out, so that σ has the same energy dependence as $1/m^*$. For Li, as implied by the DOS in Fig. 3(a), the band becomes flattened around the Fermi energy; this corresponds to an increasing effective mass. Consequently, σ decreases with energy and yields the positive sign of S.

We now turn to the possibility of doping-induced sign changes in S. If Na is electron doped we predict, using the relaxation time approach and the qualitative relation between τ and DOS, that the sign of S changes from negative to positive with a concentration $\sim 1 \times 10^{22}$ cm^{-3} (0.358 e^-/unit cell), cf. Fig. 4. This change of sign is confirmed in the VA, for slightly higher doping levels but with a much stronger amplitude: at 300 K, $S = 0.55$ μV/K from RTA while $S = 5.53$ μV/K using VA.

Clearly the proportionality between the scattering rate and DOS is qualitative, and works for simple systems. The $\tau(\epsilon)$ model fails in particular for Fermi surfaces not entirely within the first Brillouin zone. As an example, if extra electrons are added to Li, e.g., in Mg_xLi_{1-x} alloy [30], the RTA with the model $\tau(\epsilon)$ yields a change of sign of S from positive to negative at an extra electron concentration of about 8×10^{21} cm^{-3} ($Mg_{0.154}Li_{0.846}$). However, the VA-calculated S does not change sign, at least up to an added carrier concentration of 4×10^{22} cm^{-3} ($Mg_{0.771}Li_{0.229}$, which is beyond the wide range of bcc structure for the binary alloy). When the Fermi surface reaches the BZ boundary, the distortions allow additional electron-phonon scattering, which will change the scattering rate. Similar failures of the RTA with either constant or DOS-related τ are found in Cu, Ag, and Au, where the model $\tau(\epsilon)$ still gives negative S. The positive S in these group-11 metals is more complex than in Li, combining a distorted Fermi surface with nontrivial electron-phonon interactions, as was proposed by Robinson [15,16]. Fully first-principles calculations are underway to elucidate the precise mechanism.

In summary, we have calculated the first fully *ab initio* Seebeck coefficient, using a variational solution to the Boltzmann transport equation. Our calculated Seebeck coefficients of Li and Na are in good agreement with experimental data, whereas the commonly used constant relaxation time approximation fails qualitatively for Li.

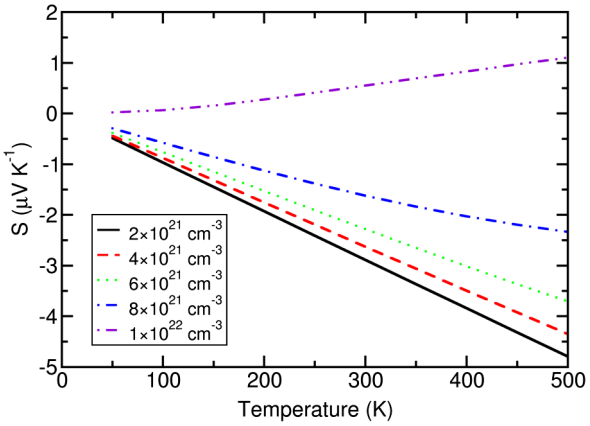

FIG. 4 (color online). Calculated Seebeck coefficient of electron-doped Na using RTA and $1/\tau(\epsilon) \propto N(\epsilon)$, as a function of temperature at several doping concentrations.

Through a comparison between Li and Na, a detailed analysis reveals that the sign of S is determined by the energy dependence of the electron lifetime (generically proportional to the inverse of the electronic DOS), whereas the quantitative influence of the electron-phonon interaction is not important. In Li, the DOS around the Fermi energy deviates considerably from the free-electron model; our analysis contradicts Robinson's earlier explanations based on exotic energy variations of the electron-phonon coupling. The possibility of tailoring the sign of the Seebeck coefficient through electronic band engineering opens many pathways to improved thermoelectric devices. In more complex cases, electron-phonon coupling effects will probably be as important as the purely electronic effects for the net variation of the electron lifetime; both are included seamlessly and on the same footing in the present formalism.

The authors thank Y. Pouillon for essential build system work on the ABINIT package. We acknowledge an A.R.C. grant (TheMoTherm Grant No. 10/15-03) and a ULg starting grant (crédit d'impulsion "Etude ab initio des transitions de phase haute température"), both from the Communauté Française de Belgique. Computer time was made available by PRACE-2IP on Huygens and Hector (EU FP7 Grant No. RI-283493), CECI, CISM-UCLouvain, and SEGI-ULg.

*Corresponding author.
bxu@ulg.ac.be

[1] M. Zebarjadi, K. Esfarjani, M. S. Dresselhaus, Z. F. Ren, and G. Chen, Energy Environ. Sci. **5**, 5147 (2012).
[2] J. Snyder and E. Toberer, Nat. Mater. **7**, 105 (2008).
[3] P. Wang and A. Bar-Cohen, J. Appl. Phys. **102**, 034503 (2007).
[4] K. Biswas, J. He, I. D. Blum, C.-I. Wu, T. P. Hogan, D. N. Seidman, V. P. Dravid, and M. G. Kanatzidis, Nature (London) **489**, 414 (2012).
[5] Y. Pei, X. Shi, A. LaLonde, H. Wang, L. Chen, and G. J. Snyder, Nature (London) **473**, 66 (2011).
[6] A. Van Herwaarden and P. Sarro, Sens. Actuators **10**, 321 (1986).
[7] V. G. Vaks, M. I. Katsnelson, V. G. Koreshkov, A. I. Likhtenstein, O. E. Parfenov, V. F. Skok, V. A. Sukhoparov, A. V. Trefilov, and A. A. Chernyshov, J. Phys. Condens. Matter **1**, 5319 (1989).
[8] C. C. Bidwell, Phys. Rev. **23**, 357 (1924).
[9] P. Kendall, Phys. Chem. Liq. **1**, 33 (1968).
[10] V. Surla, M. Tung, W. Xu, D. Andruczyk, M. Neumann, D. N. Ruzic, and D. Mansfield, J. Nucl. Mater. **415**, 18 (2011).
[11] C. L. Foiles, in *Electronic Properties • Metals: Electronic Transport Phenomena • Electrical Resistivity, Thermoelectrical Power and Optical Properties*, edited by K. H. Hellwege and J. L. Olsen, Landolt-Bornstein, New Series, Group III, Vol. 15b (Springer-Verlag, Berlin, Heidelberg, 1985).
[12] J. Ziman, *Electrons in Metals: A Short Guide to the Fermi Surface* (Taylor & Francis Group, London, 1962).
[13] D. K. C. MacDonald, *Thermoelectricity: An Introduction to the Principles* (Wiley, New York, 1962).
[14] F. J. Blatt, P. A. Schroeder, C. L. Foiles, and D. Greig, *Thermoelectric Power of Metals* (Plenum Press, New York, 1976).
[15] J. E. Robinson, Phys. Rev. **161**, 533 (1967).
[16] J. E. Robinson and J. D. Dow, Phys. Rev. **171**, 815 (1968).
[17] H. Jones, Proc. Phys. Soc. London Sect. A **68**, 1191 (1955).
[18] P. B. Allen, Phys. Rev. B **17**, 3725 (1978).
[19] S. Y. Savrasov and D. Y. Savrasov, Phys. Rev. B **54**, 16487 (1996).
[20] See Supplemental Material at http://link.aps.org/supplemental/10.1103/PhysRevLett.112.196603 for an overview of Allen's formalism; phonon dispersion curves of Li and Na; electrical resistivity of Li; Seebeck coefficient of K; and detailed analysis of the sign of the Seebeck coefficient for Li and Na.
[21] X. Gonze, Phys. Rev. B **55**, 10337 (1997).
[22] X. Gonze and C. Lee, Phys. Rev. B **55**, 10355 (1997).
[23] X. Gonze, G.-M. Rignanese, M. Verstraete, J.-M. Beuken, Y. Pouillon, R. Caracas, F. Jollet, M. Torrent, G. Zerah, M. Mikami, P. Ghosez, M. Veithen, V. Olevano, L. Reining, R. Godby, G. Onida, D. Hamann, and D. C. Allan, Z. Kristallogr. **220**, 558 (2005) [http://www.abinit.org/about/zfk_0505-06_558-562.pdf].
[24] N. Marzari, D. Vanderbilt, A. De Vita, and M. C. Payne, Phys. Rev. Lett. **82**, 3296 (1999).
[25] G. K. H. Madsen and D. J. Singh, Comput. Phys. Commun. **175**, 67 (2006).
[26] T. C. Chi, J. Phys. Chem. Ref. Data **8**, 339 (1979).
[27] M. Pozzo, C. Davies, D. Gubbins, and D. Alfe, Nature (London) **485**, 355 (2012).
[28] J. M. Ziman, *Electrons and Phonons* (Oxford University Press, New York, 1960).
[29] M. Lundstrom, *Fundamentals of Carrier Transport* (Cambridge University Press, Cambridge, England, 2009).
[30] A. Nayeb-Hashemi, J. Clark, and A. Pelton, Bull. Alloy Phase Diagrams **5**, 365 (1984).